Conformational folding induced by π–π interaction in a series of flexible dyads consisting of isomeric mesoporphyrin nitrobenzyl esters

Carles Colominas,[a] Lisbeth Eixarch,[b] Pere Fors,[b] Kamil Lang,[b,†] Santiago Nonell,[a] Jordi Teixidó[a] and Francesc R. Trull[b,*]

[a] *CETS Institut Químic de Sarrià, Universitat Ramon Llull, Via Augusta 390, E-08017 Barcelona, Catalunya, Spain*
[b] *Departament de Química Orgànica, Facultat de Química, Universitat de Barcelona, C/Martí i Franquès 1, E-08028, Barcelona, Catalunya, Spain*

A series of isomeric (*ortho*, *meta* and *para*) nitrobenzyl mono- and di-esters of mesoporphyrin, in which the nitrobenzyl group(s) is (are) mono-linked through one or both propionate chains of the porphyrin, have been synthesized and their room-temperature conformations in a number of solvents have been investigated using ^{1}H NMR spectroscopy and theoretical calculations. Folding of these flexible dyads is consistent with the following observations: (1) ^{1}H NMR ring current upfield shift in all solvents assayed [*i.e.*, $CDCl_3$, $CDCl_3$–CD_3OD (10:1) and C_6D_6] of 0.5–2.5 ppm for the aryl protons; (2) these shifts are independent of temperature over the range 25 to −55 °C; (3) the ^{1}H NMR resonance values of mesoporphyrin benzyl ester (lacking the nitro group) are not shifted, indicating a preferred, sterically less crowded, extended conformation. The presence of the nitro group on the phenyl ring(s) is responsible for the folding of these flexible dyads, and the results can be interpreted in terms of π–π interactions (C. A. Hunter and J. K. M. Sanders, *J. Am. Chem. Soc.*, 1990, 112, 5525–5534) between the two halves. In the theoretically calculated (molecular mechanics and semiempirical calculations) minimum-energy folded conformations, each benzyl group lies approximately parallel to the porphyrin π-system with its centre slightly offset relative to the centre of the porphyrin; however, for each isomer, significant structural differences between the *ortho* isomer and its *meta* and *para* counterparts are found. The implications of these differences for the photoinduced electron transfer efficiencies in these dyads are discussed.

Introduction

Rates of photoinduced electron transfer (PET) between donors (D) and acceptors (A) separated by a bridge are known to depend, among other things, on D–A distance and relative orientation. For studies of this dependence, rigid dyads are generally used.[1a,b,2] If, by contrast, the spacer binding the chromophores is flexible, then several suitable conformations are accessible depending on the presence of hindering substituents,[3] solvent and its polarity,[4] and temperature;[5] as a result, the system usually exhibits more complex behaviour.

Porphyrins are suitable for generating long-lived charge-separation species originating from their first excited singlet state. A vast number of porphyrin-based supramolecules have been developed to model the primary photochemical step of photosynthesis.[6] For similar reasons, quinones have been the acceptors of choice accompanying porphyrin donors in many of these D–A model systems.[4b,5b,6b–d,j,7] Other acceptors used include methylviologen (MV^{2+}),[4a] cyanine dyes,[6i] pyromellitimide,[8] and nitroaromatics.[9,10]

Our interest in the development of porphyrin-containing photoconductive polymeric materials based upon the principle of host–guest complexation driven by non-covalent interactions,[11] brought us to prepare several dyads consisting of a mesoporphyrin and one (or two) nitrobenzyl unit(s) connected through the porphyrin propionate chain(s). Mesoporphyrin may serve as a model for the naturally occurring porphyrins. The length and flexibility of its propionate chains are unique in that they allow the nitrobenzyl unit to explore a range of spatial dispositions around the porphyrin core, thus affording a suitable system to reveal the existence of interactions between the two units. This possibility does not occur in dyads where the propionate chain has been replaced by a shorter or more rigid linkage, as in the meso-substituted arylporphyrins. Interestingly, most artificial systems based on porphyrins studied so far belong to this second class of compounds.

In this paper, spectroscopic evidence is presented to demonstrate that such π–π interactions[12] do indeed occur, and can be exploited to facilitate the process of photoinduced electron transfer. For each isomer, a rough estimate of the geometry of the folded conformation is derived from NMR spectroscopy and a more precise picture is obtained from theoretical calculations; the abilities of the different nitrobenzyl isomers to quench fluorescence of the porphyrin are related to the relative orientation of the nitro group and porphyrin in each dyad.

Experimental

Chemicals

All solvents used in the synthesis and steady-state fluorescence measurements were of reagent grade quality, further purified by the usual procedures.[13] Dimethylformamide (99.8%, Merck) was made free of volatile amines by several cycles of evacuation and argon saturation, immediately before use; the absence of amines was confirmed with ninhydrin.[14] The deuteriochloroform (99.9% D, Merck) used in the NMR measurements was filtered through a short column of basic Al_2O_3 (activity I) immediately before sample preparation, in order to remove traces of acid. Cs_2CO_3 (99.5%, Merck) was used as a 0.04 M aqueous solution; 2-nitrobenzyl bromide, 4-nitrobenzyl bro-

† On leave from the Institute of Inorganic Chemistry, Prague, Czech Republic.

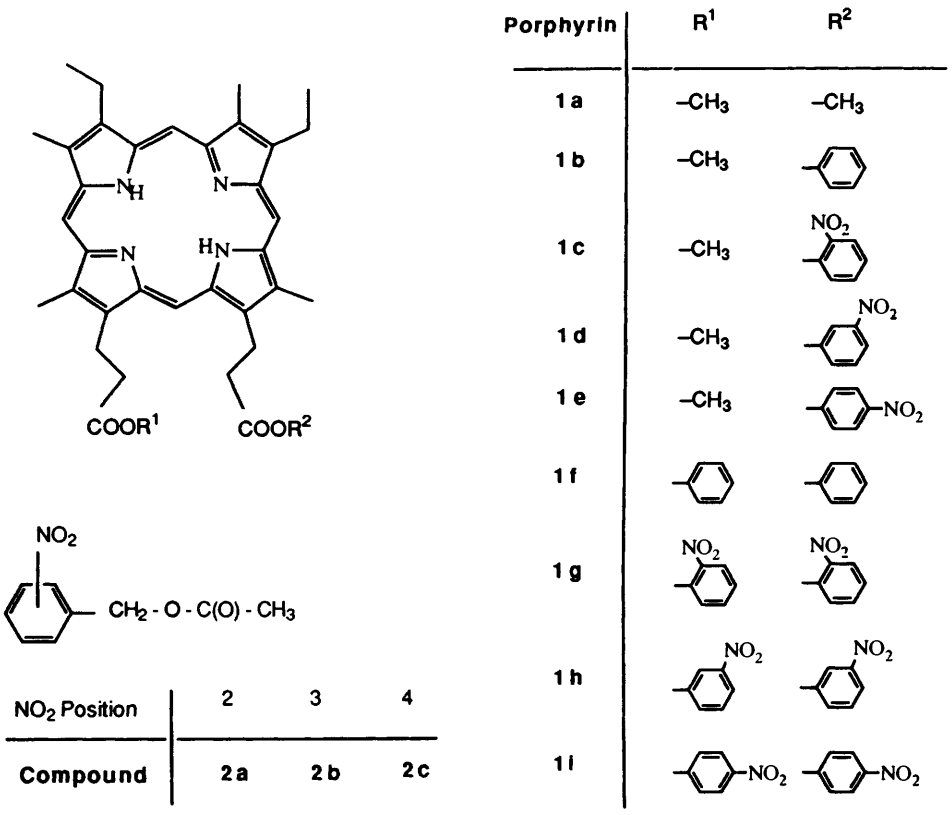

Scheme 1

mide (99%, both from Aldrich) and 3-nitrobenzyl bromide (99%, Janssen) were utilized as received. Crystalline bovine hemin (Aldrich) was used as the starting material for mesoporphyrin. The preparation of mesoporphyrin (MP) dimethyl ester, **1a**,[15a] MP monomethyl ester,[16] and MP dicaesium salt[15b] has been reported previously. Mesoporphyrin monomethyl ester monocaesium salt was prepared by neutralizing a dimethylformamide solution of mesoporphyrin monomethyl ester, with caesium acetate.[15c]

Analytical thin layer chromatography (TLC) was carried out on Merck 60 F254 silica gel plates (0.2 mm layer); flash column chromatography was performed on SDS (France) silica gel 60 (230–400 mesh). Reactions and sample manipulations were carried out in red, dim light and under argon unless otherwise specified. The purity of all porphyrins was checked by TLC on silica gel with CH_2Cl_2–CH_3OH (10:1) immediately before use and, when necessary, the samples were further purified by flash column chromatography.

Theoretical calculations

Molecular modelling, first geometry optimization and molecular dynamics-simulated annealing simulations were performed using the HYPERCHEM computer program for PC, version 3.0.[17] Rigid and relaxed conformational analysis were carried out using DDE macros developed in our laboratories[18] involving HYPERCHEM and EXCEL spreadsheets.[19] The MM+ method based on Allinger's force field was used in all molecular mechanics calculations.[20] Monte Carlo–Metropolis search[21] was performed using the MAD software package[22] on an IBM RISC/6000 workstation under AIX 3.2. Quantum-mechanical calculations were performed at the semiempirical level considering the Austin model 1 (AM1) Hamiltonian[23] of the molecular orbital package AMPAC,[24] implemented on an IBM RISC/6000.

Analytical methods

Melting points (not corrected) were determined on a Kofler–Reichert micro-hot stage apparatus. For **1c–e**, **1g–i**, the mp was in the range 135–145 °C (with decomposition). ^{1}H NMR spectra were recorded on a 200 MHz Varian-Gemini instrument. The variable temperature NMR spectra of mesoporphyrin methyl 4-nitrobenzyl ester **1e** were carried out on a 500 MHz Varian VXR500 instrument using $CDCl_3$ as the solvent; the first spectrum was recorded at 22 °C, then the sample was gradually cooled and subsequent spectra were recorded at approximately 10 °C intervals down to −55 °C. Infrared spectra were obtained on a Perkin-Elmer 681 or a Fourier-Transform Nicolet instrument. UV–VIS spectra were recorded on a Perkin-Elmer Lambda 5 or on a Shimadzu UV 2100 U spectrophotometer. Mass spectra were recorded on a Hewlett-Packard 5988-A instrument equipped for FAB analysis with a Capillaritron Frasor, using Xe as the inert gas and 1,4-dithiothreitol/dithioerytritol (DTT/DTE) as the matrix. Samples were dried overnight at 100 °C and 10 mmHg, prior to elemental analysis.

Relative fluorescence quantum yields, Φ_f

These were determined with a Perkin-Elmer LS 50 spectrofluorimeter using air-saturated benzene, CH_2Cl_2, CH_3CN and CH_3OH solutions of the porphyrin esters **1a–i**. Emission spectra were recorded exciting at the maximum of the Soret band (399 nm). Absorbances at this wavelength were optically matched ($A \leqslant 0.1$; concentrations $\leqslant 0.7$ μM). Integration of the complete fluorescence spectrum and comparison to **1a** yielded Φ_f. All spectroscopic measurements were performed at room temperature.

Nitrobenzyl acetates 2a–c

A mixture of caesium acetate (73 mg, 0.38 mmol) and the corresponding 2-, 3- or 4-nitrobenzyl bromide (17 mg, 0.08 mmol) in 3 cm^3 of dimethylformamide was allowed to react under magnetic stirring for 20 h in a water bath at 30 °C under argon. The solvent was evaporated under vacuum below 30 °C and CH_2Cl_2–H_2O (5 + 5 cm^3) was added to the residue. The organic phase was separated, washed with water (2 × 5 cm^3) and dried with Na_2SO_4. After solvent evaporation, the residue was purified by flash column chromatography eluting with CH_2Cl_2 to yield a white solid (9.6 mg, 59% yield, average)

spectroscopically identified (below) as the expected nitrobenzyl acetate.

2-Nitrobenzyl acetate (2a). Melts at room temperature; $\lambda_{max}(CH_2Cl_2)$/nm 259 (ε/dm^3 mol^{-1} cm^{-1} 10 700); ν_{max}/cm^{-1} 1750 (ester C=O), 1530, 1345 (NO_2), 1225 (C–O); $\delta_H(CDCl_3$; 200 MHz; Me_4Si) 8.1 [1 H, dd, aromatic C(3)H], 7.6 [3 H, m, aromatic C(4,5,6)H], 5.5 (2 H, s, $-CH_2-OOC-$), 2.16 (3 H, s, CH_3-COO-); $\delta_H(C_6D_6$; 200 MHz; Me_4Si) 7.54 [1 H, d, aromatic C(3)H], 7.0 [1 H, d, aromatic C(6)H], 6.81 [1 H, t, aromatic C(4)H], 6.60 [1 H, t, aromatic C(5)H], 5.27 (2 H, s, $-CH_2-OOC-$), 1.59 (3 H, s, CH_3-COO-).

3-Nitrobenzyl acetate (2b). Melts at room temperature; $\lambda_{max}(CH_2Cl_2)$/nm 261 (ε/dm^3 mol^{-1} cm^{-1} 10 900); ν_{max}/cm^{-1} 1745 (ester C=O), 1535, 1350 (NO_2), 1225 (C–O); $\delta_H(CDCl_3$; 200 MHz; Me_4Si) 8.23 [1 H, br s, aromatic C(2)H], 8.19 [1 H, d. aromatic C(4)H], 7.70 [1 H, d, aromatic C(6)H], 7.50 [1 H, t, aromatic C(5)H], 5.20 (2 H, s, $-CH_2-OOC-$), 2.15 (3 H, s, CH_3-COO-); $\delta_H(C_6D_6$; 200 MHz; Me_4Si) 7.87 [1 H, s, aromatic C(2)H], 7.69 [1 H, d, aromatic C(4)H], 6.90 [1 H, d, aromatic C(6)H], 6.62 [1 H, t, aromatic C(5)H], 4.60 (2 H, s, $-CH_2-OOC-$), 1.57 (3 H, s, CH_3-COO-).

4-Nitrobenzyl acetate (2c). Mp 73–76 °C; $\lambda_{max}(CH_2Cl_2)$/nm 266 (ε/dm^3 mol^{-1} cm^{-1} 11 000); ν_{max}/cm^{-1} 1740 (ester C=O), 1515, 1345 (NO_2), 1235 (C–O); $\delta_H(CDCl_3$; 200 MHz; Me_4Si) 8.22 [2 H, d, aromatic C(3,5)H], 7.51 [2 H, m, aromatic C(2,6)H], 5.2 (2 H, s, $-CH_2-OOC-$), 2.15 (3 H, s, CH_3-COO-); $\delta_H(C_6D_6$; 200 MHz; Me_4Si) 7.74 [2 H, d, aromatic C(3,5)H], 6.68 [2 H, m, aromatic C(2,6)H], 4.61 (2 H, s, $-CH_2-OOC-$), 1.60 (3 H, s, CH_3-COO-).

Mesoporphyrin benzyl diester 1f and nitrobenzyl diesters 1g–i

A mixture of mesoporphyrin dicaesium salt (37 mg, 0.04 mmol, 0.08 mequiv.) and either benzyl bromide or the corresponding 2-, 3- or 4-nitrobenzyl bromide (0.08 mmol) in 3 cm^3 of dimethylformamide was allowed to react, with magnetic stirring, in a water bath at 30 °C under argon. After 24 h, the solvent was evaporated off under vacuum below 30 °C and the solid residue was dissolved in CH_2Cl_2 (25 cm^3) and washed with H_2O (4 × 15 cm^3). After drying with Na_2SO_4 and solvent evaporation, the residue showed by TLC on silica gel with CH_2Cl_2–CH_3OH (10:1) mainly the expected diester (R_f *ca.* 0.8), accompanied by traces of the corresponding monoester (R_f *ca.* 0.65) and diacid (R_f = 0). Flash column chromatography eluting, in this order, with toluene, toluene–CH_2Cl_2 mixtures of increasing polarity, and CH_2Cl_2–CH_3OH mixtures, afforded pure diester (20 mg, 53% yield, average) as a reddish brown solid, identified spectroscopically.

Mesoporphyrin benzyl diester (1f). Mp 155 °C; $\lambda_{max}(CH_2Cl_2)$/nm 397 (ε/dm^3 mol^{-1} cm^{-1} 132 000), 496 (11 470), 530 (8050), 565 (5500), 619 (4000); ν_{max}/cm^{-1} 3300 (NH), 1735 (ester C=O); $\delta_H(CDCl_3$; 200 MHz; Me_4Si) 10.10 (4 H, s, meso =CH–), 7.09–7.01 (10 H, m, aromatic protons), 5.05 (4 H, s, $-CH_2-OOC-$), 4.44 (4 H, t, $-CH_2-CH_2-COO-$), 4.1 (4 H, q, $-CH_2-CH_3$), 3.65, 3.64, 3.63 (12 H, 3 × s, 4 × β–CH_3), 3.34 (4 H, t, $-CH_2-CH_2-COO-$), 1.87 (6 H, t, $-CH_2-CH_3$), −3.81 (2 H, br s, NH).

Mesoporphyrin 2-nitrobenzyl diester (1g). $\lambda_{max}(CH_2Cl_2)$/nm 264 (ε/dm^3 mol^{-1} cm^{-1} 22 300), 398 (158 600), 499 (14 000), 532 (9100), 567 (6300), 621 (3700); ν_{max}/cm^{-1} 3315 (NH), 1740 (ester C=O), 1525, 1345 (NO_2); $\delta_H(CDCl_3$; 200 MHz; Me_4Si) 10.12, 10.08, 10.07, 10.02 (4 H, 4 × s, meso =CH–), 7.5, 7.4 [2 H, 2 × d, aromatic C(3)H], 6.24 [4 H, 2 × d + 2 × t, aromatic C(4,6)H], 5.65, 5.58 [2 H, 2 × t, aromatic C(5)H], 5.33 (4 H, s, $-CH_2-OOC-$), 4.39 (4 H, t, $-CH_2-CH_2-COO-$), 4.1 (4 H, q, $-CH_2-CH_3$), 3.65, 3.62, 3.59, 3.58 (12 H, 4 × s, 4 × β–CH_3), 3.31 (4 H, t, $-CH_2-CH_2-COO-$), 1.87 (6 H, t, $-CH_2-CH_3$), −3.81 (2 H, br s, NH); $\delta_H(C_6D_6$; 200 MHz; Me_4Si) 10.17, 10.15, 10.10, 10.03 (4 H, 4 × s, meso =CH–), 6.81, 6.77 [2 H, 2 × d, aromatic C(3)H], 5.72, 5.67 [2 H, 2 × d, aromatic C(6)H], 5.23, 5.16 [2 H, 2 × t, aromatic C(4)H], 4.70, 4.60 [2 H, 2 × t, aromatic C(5)H], 5.16, 5.14 (4 H, 2 × s, $-CH_2-OOC-$), 4.24, 4.23 (4 H, 2 × t, $-CH_2-CH_2-COO-$), 3.94, 3.92 (4 H, 2 × q, $-CH_2-CH_3$), 3.39, 3.38, 3.31, 3.30 (12 H, 4 × s, 4 × β–CH_3), 3.11, 3.10 (4 H, 2 × t, $-CH_2-CH_2-COO-$), 1.82, 1.80 (6 H, 2 × t, $-CH_2-CH_3$), −3.33 (2 H, br s, NH); *m/z* (FAB) 838 (M^+ + 2) (Found: C, 69.28; H, 6.14; N, 9.69. $C_{48}H_{48}N_6O_8$ requires C, 68.88; H, 5.78; N, 10.04%).

Mesoporphyrin 3-nitrobenzyl diester (1h). $\lambda_{max}(CH_2Cl_2)$/nm 264 (ε/dm^3 mol^{-1} cm^{-1} 29 700), 399 (157 800), 498 (13 900), 532 (9200), 567 (6400), 621 (3900); ν_{max}/cm^{-1} 3500–3300 (NH), 1740 (ester C=O), 1530, 1350 (NO_2), 1155 (C–O); $\delta_H(CDCl_3$; 200 MHz; Me_4Si) 10.12, 10.06, 9.95 (4 H, 3 × s, meso =CH–), 7.8, 7.75 [2 H, 2 × s, aromatic C(2)H], 7.0, 6.85 [2 H, 2 × d, aromatic C(4)H], 6.5, 6.35 [2 H, 2 × d, aromatic C(6)H], 5.85, 5.65 [2 H, 2 × t, aromatic C(5)H], 4.92, 4.87 (4 H, 2 × s, $-CH_2-OOC-$), 4.41 (4 H, t, $-CH_2-CH_2-COO-$), 4.15 (4 H, q, $-CH_2-CH_3$), 3.67, 3.65, 3.63, 3.62 (12 H, 4 × s, 4 × β–CH_3), 3.37 (4 H, t, $-CH_2-CH_2-COO-$), 1.90 (6 H, t, $-CH_2-CH_3$), −3.94 (2 H, br s, NH); $\delta_H(C_6D_6$; 200 MHz; Me_4Si) 10.05, 9.98, 9.91, 9.87 (4 H, 4 × s, meso =CH–), 7.3, 7.2 [2 H, 2 × s, aromatic C(2)H], 6.05, 5.81 [2 H, 2 × d, aromatic C(4)H], 5.39, 5.22 [2 H, 2 × d, aromatic C(6)H], 4.45, 4.17 [2 H, 2 × t, aromatic C(5)H], 4.22, 4.15 (4 H, 2 × s, $-CH_2-OOC-$), 4.08 (4 H, t, $-CH_2-CH_2-COO-$), 3.82 (4 H, q, $-CH_2-CH_3$), 3.29, 3.27, 3.23, 3.21 (12 H, 4 × s, 4 × β–CH_3), 3.04, 3.00 (4 H, 2 × t, $-CH_2-CH_2-COO-$), 1.71, 1.70 (6 H, 2 × t, $-CH_2-CH_3$), −3.6 (2 H, br s, NH); *m/z* (FAB) 838 (M^+ + 2) (Found: C, 69.15; H, 5.58; N, 10.18. $C_{48}H_{48}N_6O_8$ requires C, 68.88; H, 5.78; N, 10.04%).

Mesoporphyrin 4-nitrobenzyl diester 1i. $\lambda_{max}(CH_2Cl_2)$/nm 268 (ε/dm^3 mol^{-1} cm^{-1} 26 000), 399 (141 300), 498 (12 000), 532 (8000), 567 (5500), 621 (3800); ν_{max}/cm^{-1} 3320–3240 (NH), 1755–1710 (ester C=O), 1520, 1350 (NO_2), 1150 (C–O); $\delta_H(CDCl_3$; 200 MHz; Me_4Si) 10.13, 10.06, 10.05, 9.99 (4 H, 4 × s, meso =CH–), 7.22, 7.19 [4 H, 2 × d, aromatic C(3,5)H], 6.61 [4 H, d, aromatic C(2,6)H], 4.88, 4.87 (4 H, 2 × s, $-CH_2-OOC-$), 4.41 (4 H, t, $-CH_2-CH_2-COO-$), 4.1 (4 H, q, $-CH_2-CH_3$), 3.65, 3.62, 3.60, 3.58 (12 H, 4 × s, 4 × β–CH_3), 3.34 (4 H, t, $-CH_2-CH_2-COO-$), 1.87 (6 H, t, $-CH_2-CH_3$), −3.81 (2 H, br s, NH); $\delta_H(C_6D_6$; 200 MHz; Me_4Si) 10.25, 10.12, 10.10, 10.04 (4 H, 4 × s, meso =CH–), 6.40, 6.36 [4 H, 2 × d, aromatic C(3,5)H], 5.56, 5.53 [4 H, 2 × d, aromatic C(2,6)H], 4.25 (4 H, s, $-CH_2-OOC-$), 4.22, 4.21 (4 H, 2 × t, $-CH_2-CH_2-COO-$), 3.97, 3.94 (4 H, 2 × q, $-CH_2-CH_3$), 3.41, 3.33, 3.31 (12 H, 3 × s, 4 × β–CH_3), 3.13 (4 H, t, $-CH_2-CH_2-COO-$), 1.87, 1.82 (6 H, t, $-CH_2-CH_3$), −3.20 (2 H, br s, NH); *m/z* (FAB) 838 (M^+ + 2) (Found: C, 69.07; H, 5.50; N, 9.78. $C_{48}H_{48}N_6O_8$ requires C, 68.88; H, 5.78; N, 10.04%).

Mesoporphyrin methyl nitrobenzyl esters 1c–e

A mixture of mesoporphyrin monomethyl ester monocaesium salt (25 mg, 0.03 mmol, 0.03 mequiv.) and the corresponding 2-, 3- or 4-nitrobenzyl bromide (16 mg, 0.07 mmol) in 4 cm^3 of dimethylformamide was allowed to react as described above for the esters **1g–i**. The mesoporphyrin methyl nitrobenzyl esters obtained, **1c–e**, with the same chromatographic behaviour as the dibenzyl esters, were purified as above, obtained in nearly quantitative yield (23 mg, 95%, average) as reddish brown solids and identified spectroscopically.

Mesoporphyrin methyl 2-nitrobenzyl ester (1c). $\lambda_{max}(CH_2Cl_2)$/nm 265 (ε/dm^3 mol^{-1} cm^{-1} 14 200), 398 (155 700), 497 (14 200), 531 (9800), 567 (6900), 620 (4600); λ_{max}(benzene)/nm 401 (ε/dm^3 mol^{-1} cm^{-1} 144 600), 498 (13 600), 530 (9000), 569 (6200), 623 (4900); $\lambda_{max}(CH_3OH$ + 5% DMSO)/nm 393 (ε/dm^3 mol^{-1} cm^{-1} 168 700), 496 (14 900), 529 (10 200), 566 (6800), 619 (4700); ν_{max}/cm^{-1} 3315 (NH), 1740 (ester C=O), 1525, 1345 (NO_2); $\delta_H(CDCl_3$; 200 MHz; Me_4Si) 10.09, 10.07, 10.05, 10.03 (4 H, 4 × s, meso =CH–), 7.45 [1 H, dd, aromatic C(3)H], 6.24 [2 H, d + t, aromatic C(4,6)H], 5.5 [1 H, dt, aromatic C(5)H], 5.32 (2 H, s, $-CH_2-OOC-$), 4.44 (2 H, t, $-CH_2-CH_2-$

$COOCH_3$), 4.34 (2 H, t, $-CH_2-CH_2-COOBz$), 4.1 (4 H, q, $-CH_2-CH_3$), 3.63 (3 H, s, $-COOCH_3$), 3.62–3.60 (12 H, 4 × s, 4 × β-CH_3), 3.4 (2 H, t, $-CH_2-CH_2-COOCH_3$), 3.2 (2 H, t, $-CH_2-CH_2-COOBz$), 1.87 (6 H, t, $-CH_2-CH_3$), −3.81 (2 H, br s, NH); δ_H(C_6D_6; 200 MHz; Me_4Si) 10.15–9.94 (4 H, 7 × s, meso =CH–), 6.64, 6.59 [1 H, 2 × d, aromatic C(3)H], 5.36, 5.34 [1 H, 2 × d, aromatic C(6)H], 4.89, 4.81 [1 H, 2 × t, aromatic C(4)H], 4.16, 4.06 [1 H, 2 × t, aromatic C(5)H], 5.06 (2 H, s, $-CH_2-OOC-$), 4.27 (2 H, m, $-CH_2-CH_2-COOCH_3$), 4.14 (2 H, m, $-CH_2-CH_2-COOBz$), 3.88 (4 H, q, $-CH_2-CH_3$), 3.30 (3 H, s, $-COOCH_3$), 3.35–3.24 (12 H, 4 × s, 4 × β-CH_3), 3.3 (2 H, t, $-CH_2-CH_2-COOCH_3$), 3.1 (2 H, t, $-CH_2-CH_2-COOBz$), 1.78, 1.77 (6 H, 2 × t, $-CH_2-CH_3$), −3.35 (2 H, br s, NH); *m/z* (FAB) 717 (M^+ + 2) (Found: C, 70.10; H, 6.02; N, 9.60. $C_{42}H_{45}N_5O_6$ requires C, 70.47; H, 6.34; N, 9.78%).

Mesoporphyrin methyl 3-nitrobenzyl ester (1d). λ_{max}(CH_2Cl_2)/nm 265 (ε/dm^3 mol^{-1} cm^{-1} 14 200), 399 (144 200), 497 (13 100), 532 (9500), 567 (7000), 620 (4900); λ_{max}(benzene)/nm 401 (ε/dm^3 mol^{-1} cm^{-1} 132 500), 499 (12 600), 531 (8700), 569 (6600), 622 (4800); λ_{max}(CH_3OH + 5% DMSO)/nm 394 (ε/dm^3 mol^{-1} cm^{-1} 141 500), 496 (14 500), 530 (10 700), 567 (7900), 619 (4900); ν_{max}/cm^{-1} 3570–3240 (NH), 1735 (ester C=O), 1530, 1350 (NO_2), 1155 (C–O); δ_H($CDCl_3$; 200 MHz; Me_4Si) 10.07, 10.06, 10.01, 10.00 (4 H, 4 × s, meso =CH–), 7.79, 7.72 [1 H, 2 × s, aromatic C(2)H], 6.95, 6.80 [1 H, 2 × d, aromatic C(4)H], 6.38, 6.27 [1 H, 2 × d, aromatic C(6)H], 5.73, 5.56 [1 H, 2 × t, aromatic C(5)H], 4.86, 4.81 (2 H, 2 × s, $-CH_2-OOC-$), 4.44 (2 H, t, $-CH_2-CH_2-COOCH_3$), 4.34 (2 H, t, $-CH_2-CH_2-COOBz$), 4.05 (4 H, q, $-CH_2-CH_3$), 3.64 (3 H, s, $-COOCH_3$), 3.63–3.58 (12 H, 4 × s, 4 × β-CH_3), 3.4 (2 H, t, $-CH_2-CH_2-COOCH_3$), 3.2 (2 H, 2 × t, $-CH_2-CH_2-COOBz$), 1.87 (6 H, t, $-CH_2-CH_3$), −3.81 (2 H, br s, NH); δ_H(C_6D_6; 200 MHz; Me_4Si) 10.10–9.89 (4 H, 5 × s, meso =CH–), 7.24, 7.17 [1 H, 2 × s, aromatic C(2)H], 5.96, 5.72 [1 H, 2 × d, aromatic C(4)H], 5.26, 5.10 [1 H, 2 × d, aromatic C(6)H], 4.25, 4.00 [1 H, 2 × t, aromatic C(5)H], 4.19, 4.13 (2 H, 2 × s, $-CH_2-OOC-$), 4.27 (4 H, m, $-CH_2-CH_2-COO-$), 3.90, 3.88 (4 H, 2 × q, $-CH_2-CH_3$), 3.36–3.21 (15 H, 8 × s, $-COOCH_3$ + 4 × β-CH_3), 3.05, 3.00 (4 H, 2 × t, $-CH_2-CH_2-COO-$), 1.80, 1.77 (6 H, 2 × t, $-CH_2-CH_3$), −3.40, −3.45 (2 H, 2 × br s, NH); *m/z* (FAB) 717 (M^+ +2) (Found: C, 70.15; H, 6.60; N, 9.93. $C_{42}H_{45}N_5O_6$ requires C, 70.47; H, 6.34; N, 9.78%).

Mesoporphyrin methyl 4-nitrobenzyl ester (1e). λ_{max}(CH_2Cl_2)/nm 269 (ε/dm^3 mol^{-1} cm^{-1} 15 600), 398 (135 400), 497 (12 600), 531 (8600), 566 (6000), 620 (4200); λ_{max}(benzene)/nm 401 (ε/dm^3 mol^{-1} cm^{-1} 143 400), 498 (13 900), 531 (9100), 569 (6200), 623 (5100); λ_{max}(CH_3OH + 5% DMSO)/nm 394 (ε/dm^3 mol^{-1} cm^{-1} 146 900), 497 (13 200), 529 (8900), 566 (6000), 618 (4400); ν_{max}/cm^{-1} 3315 (NH), 1740 (ester C=O), 1525, 1345 (NO_2); δ_H($CDCl_3$; 200 MHz; Me_4Si) 10.09, 10.08, 10.07, 10.02 (4 H, 4 × s, meso =CH–), 7.2 [2 H, s, aromatic C(3,5)H], 6.6 [2 H, d, aromatic C(2,6)H], 4.86 (2 H, s, $-CH_2-OOC-$), 4.3 (4 H, 2 × t, $-CH_2-CH_2-COO-$), 4.1 (4 H, q, $-CH_2-CH_3$), 3.67 (3 H, s, $-COOCH_3$), 3.63–3.60 (12 H, 4 × s, 4 × β-CH_3), 3.39 (2 H, t, $-CH_2-CH_2-COOCH_3$), 3.26 (2 H, t, $-CH_2-CH_2-COOBz$), 1.86 (6 H, t, $-CH_2-CH_3$), −3.8 (2 H, br s, NH); δ_H(C_6D_6; 200 MHz; Me_4Si) 10.18, 10.17, 10.15, 10.08, 10.02, 10.01, 9.94 (4 H, 7 × s, meso =CH–), 6.29, 6.26 [2 H, 2 × d, aromatic C(3,5)H], 5.45, 5.42 [2 H, 2 × d, aromatic C(2,6)H], 4.14 (2 H, s, $-CH_2-OOC-$), 4.35, 4.18 (4 H, m, $-CH_2-CH_2-COO-$), 3.92, 3.90 (4 H, 2 × q, $-CH_2-CH_3$), 3.39–3.24 (15 H, 9 × s, $-COOCH_3$ + 4 × β-CH_3), 3.16, 3.10 (4 H, 2 × t, $-CH_2-CH_2-COO-$), 1.79, 1.77 (6 H, 2 × t, $-CH_2-CH_3$), −3.22 (2 H, 2 × br s, NH); *m/z* (FAB) 717 (M^+ + 2) (Found: C, 70.75; H, 6.66; N, 9.49. $C_{42}H_{45}N_5O_6$ requires C, 70.47; H, 6.34; N, 9.78%).

Results and discussion

The mesoporphyrin (MP) nitrobenzyl monoesters **1c–e** and diesters **1g–i** can, in principle, exist in a variety of structural forms interrelated by intramolecular folding (Fig. 1). While π–π interactions[8,12,25] between the two aromatic halves are expected to favour conformations of the folded type (bottom), steric hindrance and entropic factors should favour those with an extended geometry (top). The latter should also be favoured by aromatic solvents by way of the π–π interactions between each half and the solvent molecules, competing with those between the two halves.

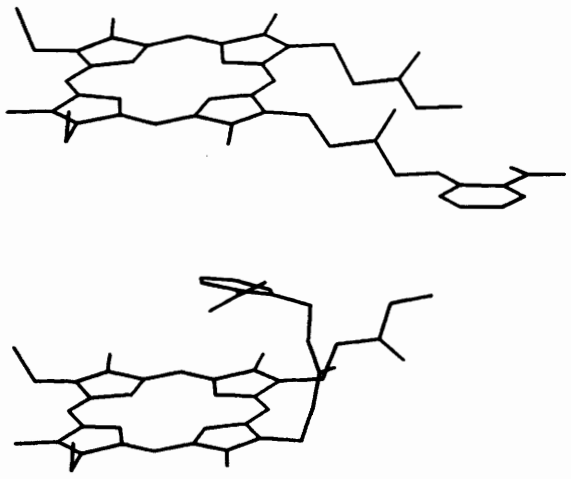

Fig. 1 AM1 geometries for mesoporphyrin 2-nitrobenzyl monoester **1c** in one of the possible minimum-energy extended (top) and folded (bottom) conformations. In the folded conformations of the nitrobenzyl diesters **1g–i**, each propionate chain is folded towards opposite sides of the porphyrin plane.

^{1}H NMR spectroscopy can be an excellent tool with which to differentiate between these extreme conformations since a predominance of folded conformations should result in the nitrobenzyl signals being shielded by the porphyrin ring current, relative to the completely extended form. The requirement for this type of treatment is that the timescale of the technique be comparable to the rate constant for conformational equilibration. If the latter process is faster, time-averaged NMR signals corresponding to the weighted populations of individual conformers are obtained.[6d,9b,9h,25] In this case, comparison of the experimental average values with those of model D–A compounds with fixed (generally by covalent bonding) folded and extended geometries, affords a useful picture of the conformational equilibrium position in the flexible dyad.

We ran a series of NMR spectra of the mesoporphyrin methyl 4-nitrobenzyl ester **1e** in $CDCl_3$ at decreasing temperatures in the range 22 to −55 °C. In contrast with a recent report on a related system,[5a] no appreciable changes were observed in the position or shape of the signals corresponding to the phenyl hydrogens. This result indicates that the observed NMR spectra must result from averaged folded and extended conformations, the folded forms being largely favoured over the entire temperature range (*e.g.*, a change of 100 : 1 to 50 : 1 would not be noticed). Table 1 shows the ^{1}H NMR chemical shifts in $CDCl_3$ and C_6D_6 for the phenyl protons of *ca.* 10^{-2} M solutions of MP nitrobenzyl monoesters **1c–e** and diesters **1g–i** as well as the respective acetates **2a–c** (in $CDCl_3$). The latter can be considered as models for chemical shifts of the nitrobenzyl signals in the absence of anisotropic effects; *i.e.*, for a completely extended geometry.

The chemical shifts of the MP nitrobenzyl monoesters **1c–e** are nearly identical with those of the corresponding diesters **1g–i**, suggesting similar conformations for both.

The only noticeable changes in chemical shifts in the MP nitrobenzyl esters **1c–e** and **1g–i** compared with reference compounds MP dimethyl ester **1a** and acetates **2a–c** concern the phenyl hydrogens. Important displacements towards higher fields are observed in the dyads (Fig. 2): indeed, the highest

Table 1 ^{1}H NMR chemical shifts (δ) for the phenyl protons of MP nitrobenzyl monoesters **1c–e**, diesters **1g–i** and acetates **2a–c** in $CDCl_3$ and C_6D_6 (in parentheses)[a]

Compound	C(2)H	C(3)H	C(4)H	C(5)H	C(6)H
2a		8.1	7.6	7.6	7.6
		(7.54)	(6.81)	(6.60)	(7.00)
2b	8.2		8.2	7.5	7.7
	(7.87)		(7.69)	(6.62)	(6.90)
2c	7.5	8.2		8.2	7.5
	(6.68)	(7.74)		(7.74)	(6.68)
1c		7.4	6.2	5.5	6.2
		(6.6)	(4.9, 4.8)	(4.2, 4.1)	(5.4)
1d	7.8, 7.7		6.9, 6.8	5.7, 5.6	6.4, 6.3
	(7.2)		(6.0, 5.7)	(4.2, 4.0)	(5.3, 5.1)
1e	7.2	6.6		6.6	7.2
	(5.4)	(6.3)		(6.3)	(5.4)
1g		7.5, 7.4	6.2	5.6	6.2
		(6.8)	(5.2)	(4.7, 4.6)	(5.7)
1h	7.8		7.0, 6.9	5.9, 5.7	6.5, 6.4
	(7.3, 7.2)		(6.0, 5.8)	(4.4, 4.2)	(5.4, 5.2)
1i	6.6	7.2		7.2	6.6
	(5.5)	(6.4)		(6.4)	(5.5)

[a] The ^{1}H NMR spectra of **1c–e** actually show pairs of close ($\Delta\delta$ < 0.2) signals for nearly all protons of the molecule. These are due to the two positional isomers [*i.e.*, 8-methyl propionate, 12-(nitrobenzyl) propionate and 8-(nitrobenzyl) propionate, 12-methyl propionate] possible. **1g–i** also show pairs of even closer ($\Delta\delta$ < 0.1) signals but only for the nitrobenzyl protons. Each set is due to one nitrobenzyl residue, the one on the 8-propionate and the one on the 12-propionate. For the sake of simplicity, we have shown only mean values of these chemical shifts.

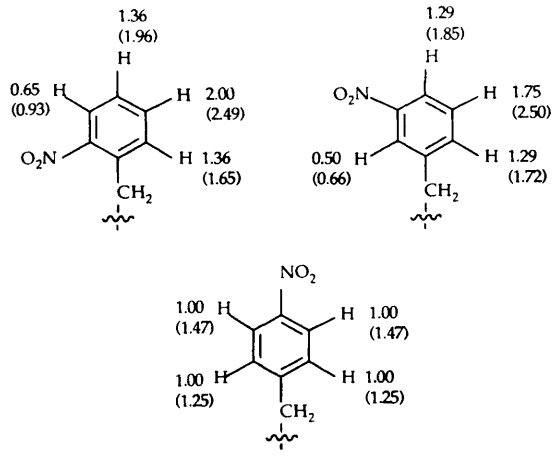

Fig. 2 Upfield ^{1}H NMR displacements ($\Delta\delta$, in ppm) of the phenyl hydrogens of MP nitrobenzyl esters **1c–e** and diesters **1g–i**, relative to the respective acetates **2a–c** in $CDCl_3$ and (in parentheses) in C_6D_6

anisotropies observed (*ca.* 2 ppm in $CDCl_3$ and *ca.* 2.5 ppm in C_6D_6) are close to those of the phenyl protons in a rigid system consisting of a porphyrin sandwiched between two parallel 2,5-dimethoxy-1,4-phenylene residues (2.33 ppm in CD_2Cl_2),[26a] or those of the pyridine protons on a so-called *ansa*-porphyrin with a pyridine in the bridge (2.5–3 ppm in [$^2H_5$]pyridine).[26b] This suggests that the conformational equilibrium in our dyads is clearly shifted to the folded side in $CDCl_3$ and C_6D_6.

In contrast with the previous results, the phenyl protons of mesoporphyrin dibenzyl ester **1f** in $CDCl_3$ appear at δ = 7.1–7.0, close to the calculated value for benzyl acetate of $\delta \approx 7.2$; *i.e.*, a predominantly extended conformation occurs in this case. This result indicates that the nitro group of MP nitrobenzyl esters is a key factor in their folding. This is in agreement with the rationale of Sanders that highly polarized π-deficient molecules form π-stacked complexes with a range of π-systems due to the reduced π-electron density at the site of π-overlap and favourable charge–charge interactions.[12] The phenomenon is quite general: while helicene, benzyl and benzoate groups covalently attached to porphyrins by flexible chains do not π-stack but prefer open conformations, π-stacking is observed between porphyrins and a wide variety of covalently attached, electron-deficient π-systems in organic solvents.[12]

In contrast with a previous report,[25c] where lower $\Delta\delta$ values were obtained in toluene rather than in chloroform, we found slightly larger anisotropies in C_6D_6. This result points, in our case, to an electrostatically driven folding. However, this conclusion must be taken with caution as benzene as a solvent is reported to behave anomalously with respect to solute complexation *vs.* dielectric constant.[27]

The upfield displacements shown by the different phenyl hydrogens of each MP nitrobenzyl ester are not equal (Fig. 2). In the 2-nitro- and 3-nitro-benzyl isomers, the largest change is shown by C(5)H ($\Delta\delta \approx 1.75$–2), followed by C(4)H and C(6)H ($\Delta\delta \approx 1.29$–1.36), and by C(2)H (in the 3-nitro isomer, $\Delta\delta \approx 0.5$) and C(3)H (in the 2-nitro isomer, $\Delta\delta \approx 0.65$). The MP-ring-current induced field opposes the external field (and therefore results in resonances at higher field) above and below the area defined by the macrocycle skeleton, and its magnitude is stronger in the centre. Hence, although the above anisotropies do not permit us precisely to establish the time-averaged phenyl-to-porphyrin orientation, they indicate that in the 2-nitro- and 3-nitro-benzyl isomers, it must be similar. In addition, in the 2-nitro and 3-nitro isomers, rapid flipping of the nitrophenyl substituent can occur (see below the theoretically calculated low energy barrier associated with this process) which interconverts the two extreme folded conformations, *i.e.*, with the nitro group towards the porphyrin centre or away from it. Therefore, the distinct anisotropies found for the several phenyl protons (above and Fig. 2) could be due either to the preference for one face rather than the other to be stacked on the porphyrin, or to the different position in each of them of the nitrophenyl ring, relative to the porphyrin macrocycle, or to a combination of the two. The particular numerical values of the anisotropies [*i.e.*, similar numbers for C(4)H and C(6)H in the 2-nitro- and 3-nitro-benzyl esters, the highest value obtained for C(5)H and the lowest for C(2)H and C(3)H] are compatible with time-averaged geometries in which the nitrophenyl group is offset relative to the porphyrin macrocycle, with the nitro group, C(2)H and C(3)H preferentially oriented towards the periphery of the porphyrin, while (especially) C(5)H and (less so) C(4)H and C(6)H are directed towards the centre. An offset geometry is most likely associated with optimum π–π

Table 2 Relative enthalpies of formation $\Delta H°_f$ (from semiempirical calculations) and minimum-energy geometries for the folded and extended conformations of MP methyl nitrobenzyl esters **1c–1e** and model acetates **2a–c**

Compound	$\Delta H°_f$/ kcal mol^{-1}	NO_2–Phenyl dihedral angle	r_{DA}/Å
2a	−62.35	−9°	—
2b	−63.96	−4°	—
2c	−64.29	0°	—
1c, folded	19.72	40°	5.47
1d, folded	18.06	0°	5.84
1e, folded	18.94	4°	5.93
1c, extended	19.92	6°	11.87
1d, extended	19.91	1°	12.09
1e, extended	19.61	0°	12.08

interactions in these systems.[12] In the case of the 4-nitrobenzyl isomer, of course, the two faces are identical by symmetry so C(3)H and C(5)H must be equivalent. The precise nitro-to-phenyl dihedral angle (and the corresponding relative orientation of nitro group to MP) in each isomer cannot be unequivocally deduced from NMR spectroscopy either, although one might expect that an *ortho*-substituent would influence the orientation of the nitro group.

The absorption spectra of *ca.* 10^{-6} M solutions of the mesoporphyrin nitrobenzyl esters **1c–e** and **1g–i** show minor differences with respect to the simple sum of that of the mesoporphyrin chromophore (*i.e.*, **1a**) plus the respective 2-, 3- or 4-nitrobenzyl acetate **2a–c**. A slight red shift (1–4 nm) in the position of the Soret band (but not of the Q bands) of the dyads, and a concomitant broadening (3–8 nm at half maximum) can be observed for the three isomers. These effects are moderately solvent dependent, with the largest differences being observed in methanol and the largest band broadening in benzene. These results are in excellent agreement with those reported for an aromatic-bridged porphyrin dimer, where the folded conformation is controlled by π–π interactions; the UV–VIS absorption spectrum has been reported to be simply the sum of the spectra of the different aromatic components,[8a] thus reinforcing the conclusion of occurrence of folded forms with a small degree of π-system distortion.

Molecular mechanics and semiempirical calculations carried out on ground state 2-, 3- and 4-nitrobenzyl acetates, **2a–c**, mesoporphyrin dibenzyl ester **1f**, dyads **1c–e** and triad **1g** provide a detailed picture of the geometries of the dyads as well as theoretical support for the assumptions made on the basis of ^{1}H NMR and UV–VIS data. Beginning with several of the possible extended conformations, MM+ molecular dynamics simulations, Monte Carlo Metropolis search on the propionate chains and simulated annealing yielded folded conformations for **1c–e** in all cases. However, MM+ calculations also predicted folded conformations as more stable for MP dibenzyl ester **1f** (no nitro group), in contrast with the ^{1}H NMR evidence. These results indicate that MM+ calculations overestimate the contribution to folding of the dyads by the intramolecular forces considered in these calculations, a conclusion in agreement with the claim by Sanders[12] that the results of MM+ calculations should be taken with caution when applied to systems with interacting aromatic groups, since they do not allow for the spatial charge distribution of the π-electron system. AM1 semiempirical calculations have been used to optimize the geometries of these systems to an energy minimum and to compare their respective formation enthalpies. For folded conformations, centre-to-centre (porphyrin-to-nitrobenzyl) distances of about 6 Å were found, in agreement with the weak molecular orbital distortions suggested by UV–VIS. For the extended conformations, the centre-to-centre distances are of about 12 Å. The differences of AM1 enthalpies (Table 2) for stand alone 'in vacuo' systems do not point to any preferred (folded or extended) conformation.

For MP methyl nitrobenzyl esters **1c–e**, two nearly isoenergetic folded conformations were found upon varying the position of the methyl propionate chain from the same side — relative to the nitrobenzyl propionate — of the macrocycle plane to the opposite side. Folded conformations were also found for MP 2-nitrobenzyl diester **1g**, with the two aryl propionate chains oriented towards opposite sides of the porphyrin macrocycle.

Two conformational studies were carried out on the folded dyads **1c–e**: one on the rotation of the nitrophenyl ring around the $Ph(NO_2)$–CH_2 bond and the other on both the nitro torsion angle and the acetate chain torsion angle in the nitrobenzyl acetates **2a–c**. The MM+ rotational study on the $Ph(NO_2)$–CH_2 bond of folded **1c–e** reveals similar behaviour for *o*-nitro and *m*-nitro isomers but very different for *p*-nitro isomers, as one would anticipate, and consistent with the structural features derived from the ^{1}H NMR results: when the nitro group is in *ortho*- or *meta*-positions, the overall (360°) rotational barrier is higher than 15 kcal mol^{-1} (MM+), but only 1 kcal mol^{-1} in the *p*-nitro isomer. The half-way low rotational barrier (*ca.* 200°, NO_2 up away from the porphyrin) is lower than 3 kcal mol^{-1} in all cases, and leads, for *ortho*- or *meta*-isomers, to two nearly isoenergetic broad minima. Qualitatively, this analysis shows that multiple energetically similar conformations can exist for each dyad even in the folded geometry. As expected, potential energy surfaces obtained from rigid and relaxed conformational analysis on the nitrobenzyl acetates **2a–c** show a clear dependence between nitro group torsion angle and acetate chain torsion angle for 2- but not for 3- or 4-nitrobenzyl acetates. For the *ortho* isomer, the potential energy surface shows various minima around 20° and 240° acetate torsion angles, all of them corresponding to non-coplanar nitro and phenyl ring. For the *meta* and *para* isomers the nitro group is nearly coplanar to the phenyl ring.

Consistent with this, AM1 calculations on nitrobenzyl acetates **2a–c**, and dyads **1c–e** (*cf.*, Table 2) show for the *meta*- and *para*-nitro isomers, values of nitro-to-phenyl dihedral angles lower than 4°. In the *ortho*-nitro isomers, this angle is 6–9° for 2-nitrobenzyl acetate, **2a**, and the extended conformation of dyad **1c**, but—more interestingly—40° for its folded conformation. In this case, the folding of the propionate chain binding nitrobenzyl and porphyrin restrains the propionate-to-phenyl torsion angle to −120°, and this in turn forces the nitro-to-phenyl torsion angle to move towards one of the local minima of the energy surface.

Fluorescence spectra and yields in the linked systems

The kinetics of electron transfer between donor (D) and acceptor (A) are known to depend strongly on the D–A separation distance. This has been nicely shown in a recent report on photoinduced electron transfer in a dyad consisting of $Re(CO)_3(bpy)(py)^+$ connected to nitrobenzene by a flexible crown-ether-based link.[5a] Changing the temperature of the system produced changes in the electron transfer rate constant that the authors ascribed to a modulation of the equilibrium between open and folded forms.[5a] We thus decided to investigate PET in our flexible dyads through the quenching of the porphyrin fluorescence.

The fluorescence emission spectra of *ca.* 10^{-6} M CH_2Cl_2 solutions of MP nitrobenzyl mono- and di-esters **1c–e** and **1g–i** have the same shape as that of the dimethyl ester, **1a**, with the maximum at 622 nm. In benzene, a small bathochromic shift to 625 nm occurs but no new bands are observed. Excitation spectra are also basically identical in all cases and equal to the respective absorption spectra. These observations indicate that no significant alteration of the first excited singlet *vs.* ground state geometries of the porphyrin skeleton has occurred in the dyads relative to **1a**.

Table 3 Relative fluorescence quantum yields, Φ_f, and PET rate constants, k_{ET}, in air-saturated CH_2Cl_2 for the model porphyrins **1a**, **1f**, dyads **1c–e** and triads **1g–i**

Porphyrin	Φ_f[a]	k_{ET} (10^8 s^{-1})[b]
1a	1	—
1c	0.58	0.68
1d	0.31	2.1
1e	0.33	1.9
1f	0.96	—
1g	0.42	1.3
1h	0.18	4.3
1i	0.20	3.8

[a] From steady-state fluorescence; relative to **1a**, errors ± 10%; samples of $A_{399} = 0.1$; $\lambda_{exc} = 399$ nm. [b] Using the equation $k_{ET} = (1 - \Phi_f)/\tau_f^{1a}\Phi_f$, with $\tau_f^{1a} = 10.5$ ns being the fluorescence lifetime of **1a**.

The fluorescence quantum yields, Φ_f — relative to **1a** — for **1c–e** and **1g–i** in air-saturated CH_2Cl_2 are shown in Table 3. The two nitro-free porphyrins **1a**, **1f** show the same Φ_f (no effect by the benzyl groups), whereas the presence of a nitro group on the phenyl ring decreases Φ_f, indicating an additional fast deactivation process. This is identified as an intramolecular PET process originating from the donor first excited singlet, by analogy to similar observations for related porphyrin-(poly)-nitrobenzene[4b,7c,9,15c] and porphyrin-quinone[2a,4b,5b,6b–d,6j,7] dyads. In a non-linked system consisting of 1 μM mesoporphyrin dimethyl ester and 1 μM nitrobenzyl acetate (any of the three isomers) no reduction of the porphyrin fluorescence intensity could be observed. This confirms the intramolecular nature of the quenching process in the dyads.

As expected, the decrease in Φ_f values is larger in the porphyrins substituted by two nitrobenzyl residues. For the two series of compounds, it is isomer dependent, with the 3- and 4-nitrobenzyl isomers showing similar Φ_f values and clearly lower than the 2-nitrobenzyl derivatives. This corresponds to a more efficient PET process in the 3- and 4-nitrobenzyl isomers, behaviour that correlates with the less favourable nitro-to-phenyl relative orientation theoretically calculated for the 2-nitrobenzyl isomer in its folded conformation.

The ultimate goal of the present work is to construct flexible porphyrin-based photoconductive polymeric systems in which the desired orientation between adjacent chromophores is achieved by non-covalent interactions of the type discussed here. Further work is in progress along this line.

Acknowledgements

This work is part of the CICYT research program MAT91-0901-C03-01. Financial support to P. F. and to K. L. from the Spanish *Ministerio de Educación y Ciencia* is acknowledged. S. N. thanks the *Max-Planck-Gesellschaft* for an Otto Hahn fellowship. Thanks are due to Professor S. E. Braslavsky (*MPI für Strahlenchemie*, Mülheim/Rühr, Germany) for comments and encouragement.

References

1 (*a*) M. R. Wasielewski, *Photoinduced Electron Transfer*, eds. M. A. Fox and M. Chanon, Elsevier, Amsterdam, 1988, Part A, p. 161; (*b*) N. Sutin, *Electron Transfer in Inorganic, Organic, and Biological Systems*, eds. J. R. Bolton, N. Mataga and G. McLendon, Advances in Chemistry Series 228, ACS, Washington, 1991, p. 25.

2 (*a*) M. R. Wasielewski and M. P. Niemczyk, *J. Am. Chem. Soc.*, 1984, **106**, 5043; (*b*) H. Oevering, M. N. Paddon-Row, M. Heppener, A. M. Oliver, E. Cotsaris, J. W. Verhoeven and N. S. Hush, *J. Am. Chem. Soc.*, 1987, **109**, 3258.

3 A. Osuka, K. Maruyama and S. Hirayama, *Tetrahedron*, 1989, **45**, 4815.

4 (*a*) Y. Kanda, H. Sato, T. Okada and N. Mataga, *Chem. Phys. Lett.*, 1986, **129**, 306; (*b*) J. Liu, J. A. Schmidt and J. R. Bolton, *J. Phys. Chem.*, 1991, **95**, 6924.

5 (*a*) C. A. Berg-Brennan, D. I. Yoon and J. T. Hupp, *J. Am. Chem. Soc.*, 1993, **115**, 2048; (*b*) L. R. Khundkar, J. W. Perry, J. E. Hanson and P. B. Dervan, *J. Am. Chem. Soc.*, 1994, **116**, 9700.

6 (*a*) R. R. Bucks, T. L. Netzel, I. Fujita and S. G. Boxer, *J. Phys. Chem.*, 1982, **86**, 1947; (*b*) T. A. Moore, D. Gust, P. Mathis, J.-C. Mialocq, C. Chachaty, R. V. Bensasson, E. J. Land, D. Doirit, P. A. Liddell, W. R. Lehman, G. A. Nemeth and A. L. Moore, *Nature (London)*, 1984, **307**, 630; (*c*) D. Gust, T. A. Moore, L. R. Makings, P. A. Liddell, G. A. Nemeth and A. L. Moore, *J. Am. Chem. Soc.*, 1986, **108**, 8028; (*d*) D. Gust, T. A. Moore, P. A. Liddell, G. A. Nemeth, L. R. Makings, A. L. Moore, D. Barrett, P. J. Pessiki, R. V. Bensasson, M. Rougée, C. Chachaty, F. C. De Schriver, M. Van der Auweraer, A. R. Holzwarth and J. S. Connolly, *J. Am. Chem. Soc.*, 1987, **109**, 846; (*e*) R. M. Hermant, P. A. Liddell, S.-Lin, R. G. Alden, H. K. Kang, A. L. Moore, T. A. Moore and D. Gust, *J. Am. Chem. Soc.*, 1993, **115**, 2080; (*f*) J.-C. Chambron, A. Harriman, V. Heitz and J.-P. Sauvage, *J. Am. Chem. Soc.*, 1993, **115**, 6109; (*g*) J.-C. Chambron, A. Harriman, V. Heitz and J.-P. Sauvage, *J. Am. Chem. Soc.*, 1993, **115**, 7419; (*h*) S. Prathapan, T. E. Johnson and J. S. Lindsey, *J. Am. Chem. Soc.*, 1993, **115**, 7519; (*i*) J. S. Lindsey, P. A. Brown and D. A. Siesel, *Tetrahedron*, 1989, **45**, 4845; (*j*) M. R. Wasielewski, *Chem. Rev.*, 1992, **92**, 435.

7 (*a*) A. R. McIntosh, A. Siemiarczuk, J. R. Bolton, M. J. Stillman, T.-F. Ho and A. C. Weedon, *J. Am. Chem. Soc.*, 1983, **105**, 7215; (*b*) A. Siemiarczuk, A. R. McIntosh, T.-F. Ho, M. J. Stillman, K. J. Roach, A. C. Weedon, J. R. Bolton and J. S. Connolly, *J. Am. Chem. Soc.*, 1983, **105**, 7224; (*c*) M. C. González, A. R. McIntosh, J. R. Bolton and A. C. Weedon, *J. Chem. Soc., Chem. Commun.*, 1984, 1138; (*d*) J. R. Bolton, T.-F. Ho, S. Liauw, A. Siemiarczuk, C. S. K. Wanand and A. C. Weedon, *J. Chem. Soc., Chem. Commun.*, 1985, 559; (*e*) A. Osuka, S. Morikawa, K. Maruyama, S. Hirayama and T. Minami, *J. Chem. Soc., Chem. Commun.*, 1987, 359; (*f*) Y. Aoyama, M. Asakawa, Y. Matsui and H. Ogoshi, *J. Am. Chem. Soc.*, 1991, **113**, 6233; (*g*) T. Hayashi, T. Miyahara, N. Hashizume and H. Ogoshi, *J. Am. Chem. Soc.*, 1993, **115**, 2049; (*h*) Y. Kuroda, M. Ito, T. Sera and H. Ogoshi, *J. Am. Chem. Soc.*, 1993, **115**, 7003; (*i*) A. Osuka and K. Maruyama, *Tetrahedron*, 1989, **45**, 4815.

8 (*a*) H. L. Anderson, C. A. Hunter, N. M. Meah and J. K. M. Sanders, *J. Am. Chem. Soc.*, 1990, **112**, 5780; (*b*) R. J. Harrison, B. Pearce, G. S. Beddard, J. A. Cowan and J. K. M. Sanders, *Chem. Phys.*, 1987, **116**, 429.

9 (*a*) G. R. Seely, *J. Phys. Chem.*, 1972, **76**, 172; (*b*) B. G. Maiya and V. Krishnan, *J. Phys. Chem.*, 1985, **89**, 5225 and references therein; (*c*) G. R. Seely, *Tetrahedron*, 1989, **45**, 4729; (*d*) F. D'Souza and V. Krishnan, *Photochem. Photobiol.*, 1990, **51**, 285; (*e*) D. Gust, T. A. Moore, D. K. Luttrull, G. R. Seely, E. Bittersmann, R. B. Bensasson, M. Rougée, E. J. Land, F. C. De Schriver and M. Van der Auweraer, *Photochem. Photobiol.*, 1990, **51**, 419; (*f*) F. D'Souza and V. Krishnan, *Photochem. Photobiol.*, 1992, **56**, 145; (*g*) C. Turró, C. K. Chang, G. E. Leroi, R. I. Cukier and D. G. Nocera, *J. Am. Chem. Soc.*, 1992, **114**, 4013; (*h*) M. Sirish and B. G. Maiya, *J. Photochem. Photobiol. A*, 1994, **77**, 189.

10 J. S. Connolly, *Photochemical Conversion and Storage of Solar Energy-1982*, ed. J. S. Rabani, Weizmann, Jerusalem, 1982, Part A, p. 175.

11 M. A. Fox, *Acc. Chem. Res.*, 1992, **25**, 569, and references therein.

12 C. A. Hunter and J. K. M. Sanders, *J. Am. Chem. Soc.*, 1990, **112**, 5525.

13 (*a*) J. A. Riddick and W. B. Bunger, *Techniques of Chemistry. Vol. 2. Organic Solvents*, ed. A. Weissberger, Wiley Interscience, New York, 1970; (*b*) D. D. Perrin, D. R. Perrin and W. L. F. Armarego, *Purification of Laboratory Chemicals*, Pergamon, Oxford, 1980.

14 V. K. Sarin, J. B. H. Kent, J. B. Tam and R. B. Merrifield, *Anal. Biochem.*, 1981, **117**, 147.

15 (*a*) J. M. Ribó, M. L. Sesé and F. R. Trull, *React. Polym.*, 1989, **10**, 239; (*b*) P. Castán, J. M Ribó and F. R. Trull, *React. Polym.*, 1988, **9**, 237; (*c*) S. Nonell, M. L. Sesé, D. O. Mártire, S. E. Braslavsky and F. R. Trull, *Photochem. Photobiol.*, 1991, **53**, 185.

16 M. Fontich, P. Fors, M. L. Sesé and F. R. Trull, *Eur. Polym. J.*, 1994, **30**, 1143.

17 HYPERCHEM, v. 3.0 1993, Autodesk Inc.

18 SCANTOR 1994, Excel 4.0 macro developed by J. Sedó, *Institut Químic de Sarrià*, Barcelona.

19 MICROSOFT EXCEL, v. 4.0a 1992, Microsoft Corporation.

20 (*a*) HYPERCHEM *User's Manual*; Autodesk Inc. 1992; (*b*) N. L. Allinger, *J. Am. Chem. Soc.*, 1977, **99**, 8127; (*c*) N. L. Allinger and Y. H. Yoh, *QCPE Bull.*, 1980, **12**, 395; (*d*) O. Burkett and N. L. Allinger, *Molecular Mechanics*; ACS Monograph Series 177; American Chemical Society, Washington DC, 1982.

21 N. Metropolis and A. W. Rosenbluth, *J. Chem. Phys.*, 1953, **21**, 1087.

22 Molecular Advanced Design, v. 2.12 Oxford Molecular X-Pole-Ecole Polytechnique, F-91128 Palaiseau Cédex, France, 1993.
23 M. J. S. Dewar, E. G. Zoebisch, E. F. Healy and J. J. P. Stewart, *J. Am. Chem. Soc.*, 1985, **107**, 3902.
24 AMPAC from MOTECC-91, v. 2.10, D. A. Liotard, E. F. Healy, J. M. Ruiz and M. J. S. Dewar, 1991.
25 (*a*) M. D. Bentley and M. J. S. Dewar, *Tetrahedron Lett.*, 1967, **50**, 5043; (*b*) G. M. Sanders, M. van Dijk, A. van Veldhuizen and H. C. J. van der Plas, *J. Chem. Soc., Chem. Commun.*, 1986, 1311; (*c*) G. M. Sanders, M. van Dijk, A. van Veldhuizen, H. C. J. van der Plas, U. Hofstra and T. J. Schaafsma, *J. Org. Chem.*, 1988, **53**, 5272; (*d*) C. A. Hunter, M. N. Meah and J. K. M. Sanders, *J. Am. Chem. Soc.*, 1990, **112**, 5773.
26 (*a*) J. Weiser and H. A. Staab, *Angew. Chem., Int. Ed. Engl.*, 1984, **23**, 623; (*b*) C. Ohm and E. Breitmaier, *J. Prakt. Chem.*, 1994, **376**, 530.
27 P. Laszlo, *Prog. NMR Spectrosc.*, 1967, **3**, 231.

Paper 5/03998C
Received 1*st October* 1995
Accepted 17*th November* 1995